PROPERTIES OF NANOCRYSTALLINE FE-NI PARTICLES PREPARED BY THERMAL REDUCTION OF OXALATE PRECURSORS

[1]Eva ŠVÁBENSKÁ, [1,2]Pavla ROUPCOVÁ, [1,2]Lubomír HAVLÍČEK, [1]Oldřich SCHNEEWEISS

[1]Institute of Physics of Materials, Czech Academy of Science, Brno, Czech Republic, EU,
svabenska@ipm.cz

[2]CEITEC Brno University of Technology, Brno, Czech Republic, EU

https://doi.org/10.37904/nanocon.2023.4773

Abstract

Recent technological advancements require development of cost-effective and high-performance magnets which ideally do not contain rare earth metals or noble metals. The promising candidates are Fe-Ni-based alloys, in particular, the $Fe_{50}Ni_{50}$ $L1_0$ phase (tetrataenite), which has a great perspective for producing hard magnetic materials. Our study explores a promising method for preparing nanoparticles of Fe-Ni alloy from an iron-nickel oxalate precursor. The coprecipitation method was employed to prepare oxalate precursors, followed by controlled thermal decomposition in a reducing hydrogen atmosphere. The morphology and properties of the resulting particles were analysed using scanning electron microscopy (SEM) coupled with energy dispersive X-ray spectroscopy (EDX), X-ray diffraction (XRD), Mössbauer spectroscopy (MS), and magnetic measurements.

The SEM analysis revealed that the particles have approximately cube-shaped unit cell morphology with a size in a range of 1 - 2 μm. Upon annealing, the samples contain multiple phases with varying Fe-Ni content. Magnetic measurements confirmed the formation of magnetically suitable Fe-Ni phases in the samples after annealing. Mössbauer spectroscopy emerged as a highly effective method for characterizing individual phases of the Fe-Ni system.

Keywords: Magnetic materials, thermal decomposition, Mössbauer spectroscopy

1. INTRODUCTION

Magnetic materials have significantly propelled development of our civilization since their discovery. Hard magnetic materials, characterized by high coercivity (Hc), high saturation magnetization (Ms), and large peak products $(BH)_{max}$ find wide applications across various fields. The market of permanent magnets is divided with approximately one-half dominated by ferrites and the other half mainly represented by rare-earth elements (REEs) based hard magnets [1]. Ferrites have proved suitable for applications with various power density requirements. Magnetic devices that require large magnetic anisotropy and large coercivity contain magnets based on REEs such as Nd. However, REEs magnets have two main disadvantages - a low Curie temperature (~300 °C) and geo-political limitations of sources associated with the possible rapid depletion of REEs resources [1,2]. Fortunately, the $L1_0$ FeNi emerges as a promising alternative to REE-based permanent magnets.

The $L1_0$-ordered FeNi phase, known as tetrataenite, has been identified in meteorites and terrestrial rocks [3-5]. The properties that made $L1_0$ FeNi such attractive as a substitute for REE-based permanent magnets are the high magnetic anisotropic energy (Ku), magnetic saturation (Ms) value, and a large value of energy density $(BH)_{max}$. However, these values vary depending on the source (various meteorites) or the method of preparation of tetrataenite [1,6]. Many different methods of preparing the $L1_0$-FeNi phase can be found in the literature with varying degrees of success. Some involve treating FeNi alloy with neutron irradiation [7,8], high-

pressure torsion [9], cryo-milling [10], or high-energy ball milling [11]. Other methods of preparing the $L1_0$-FeNi phase are based on the information obtained from the study of meteorites. Crystallization or casting at specific conditions was reported by Goldstein, Sato, Kim, and Ivanov [3,12-14]. Another method involves annealing a predominantly nanocrystalline precursor in different atmospheres and at different temperatures. Experiments with an annealing temperature around 320 °C and using a hydrogen atmosphere appear to be the most promising [15,16]. In this work, we applied a modified procedure of synthesis of Fe-Ni phases to prepare hard magnetic materials.

2. MATERIALS AND METHODS

2.1 Materials

Iron(II) sulphate heptahydrate, nickel sulphate hexahydrate, and oxalic acid dihydrate were purchased from Penta Ltd. All the reagents were of analytical grade.

2.2 Preparation of oxalate precursors

The oxalate precursors were synthesized via the coprecipitation method, following this procedure: The homogeneous solutions of ferrous sulphate heptahydrate, nickel sulphate hexahydrate (both with a concentration of 0.5 mol/l) and oxalate acid (1 mol/l) were prepared by dissolving in an equal volume of distilled water. Solutions of nickel sulphate and ferrous sulphate were added dropwise to the oxalic acid solution with constant stirring. The solution was stirred for about 15 min, then the precipitate was isolated by filtration, washed several times with ethanol, and dried. The oxalate precursor was characterized by microscopy, powder X-ray diffraction (XRD), and Mössbauer spectroscopy (MS).

2.3 Thermal decomposition

Thermal decomposition product was prepared by annealing of oxalate precursor sample for 20 h in laboratory furnace in a hydrogen atmosphere.

2.4 Characterization methods

A TESCAN LYRA 3XMU FEG/SEM scanning electron microscope equipped with an XMax80 Oxford Instruments detector for energy dispersive X-ray analysis (EDS) was used to follow the chemical composition. The secondary electron (SE) images and energy dispersive X-ray spectra (EDS) were obtained at 12 kV and 15 kV accelerating voltage, respectively. The phase compositions study was carried out with an Empyrean diffractometer (Panalytical) in the Bragg-Brentano geometry with CoKα radiation (λ = 0.17902 nm) at room temperature (RT). The analysis of patterns was realized by HighScore® software and the ICDD (PanAnalytical) database. The ^{57}Fe Mössbauer spectra were measured at room temperature using a ^{57}Co (Rh) source in transmission geometry with a 14.4 keV gamma radiation (MS) detection using a standard Mössbauer spectrometer. A pure α-Fe foil was used as a calibration standard for the velocity scale. The computer processing of detected spectra was done using the CONFIT program package [17]. Magnetic properties were measured with the EverCool II PPMS (Quantum Design) system using a VSM mode in the temperature range of 4-300 K and with the magnetic field range of - 9T to + 9T.

3. RESULTS AND DISCUSSION

3.1 Characterization of precursor

The morphology of $Fe_{(1-x)}Ni_xC_2O_4$ particles was examined by SEM. Results are shown in **Figure 1a**. Particles of $Fe_{(1-x)}Ni_xC_2O_4$ have a rectangle shape with uniform size in the range of 1.5 - 2 μm. Based on EDS analysis,

the relative proportions of iron and nickel in the prepared oxalate precursor were determined to be 48% and 52% by weight, respectively.

Table 1 Hyperfine parameters resulting from the Mössbauer spectra analysis of oxalate precursors (IS - isomer shift, QS_{pl} - quadrupole splitting, A - phase content in atomic fraction of Fe).

Component	IS (mm/s)	QS_{pl} (mm/s)	A
D1	1.218±0.006	1.67±0.01	0.42±0.01
D2	1.045±0.024	1.98±0.04	0.35±0.01
L	0.306±0.013		0.23±0.01

Mössbauer spectra of the precursors are composed of two quadrupole doublets and one singlet with hyperfine parameters listed in **Table 1**. The first doublet shows isomer shift IS = 1.21 ± 0.01 mm/s and quadrupole splitting QS_{pl} = 1.76±0.02 mm/s consistent with high-spin Fe(II). This result agrees with the data reported in [18,19]. The second doublet has IS = 1.04 ± 0.02 mm/s and QS_{pl} = 1.98±0.04 mm/s. This corresponds with QS reported for metal mixed oxalates Fe-Ni, see, e.g., Ref. [20]. The singlet with IS=0.30±0.01 mm/s corresponds to fine particles. The phase content in the atomic fraction of Fe is 0.42 for D1, 0.35 for D2 and 0.23 for L1.

Several XRD patterns of the precursor were evaluated as iron oxalate dihydrate-$FeC_2O_4.2H_2O$ with a particle size of about 30 nm. The possible reason for these results is the substitution of some ions and/or superposition of patterns because of nearly identical positions of diffraction peaks in iron and nickel oxalates patterns (ICSD 161344 and 150590), which cannot be distinguished.

3.2 Characterization of the thermal decomposition product

The result of the thermal decomposition of the oxalate precursors in a hydrogen atmosphere was a porous structure of the particles (**Figure 1b**). Thermal decomposition led to a fine reduction size of particles (1.2 - 1.5 μm).

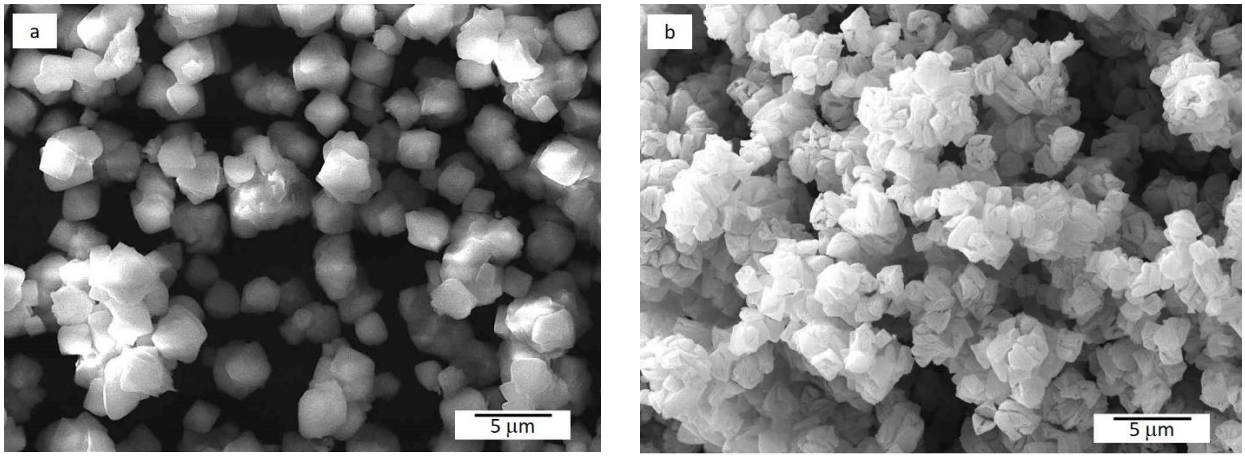

Figure 1 SEM images of morphological changes (a) oxalate precursor as starting material; (b) FeNi powder after thermal decomposition.

The representation of metals iron and nickel according to EDS analysis was the same as in the case of the precursor. XRD pattern shows (**Figure 2**) two cubic phases, namely the major fcc iron-nickel austenite (98 wt.%; a=0.3583 nm; ICSD 163354) and bcc ferrite (2 wt.%; a=0.2871 nm; ICSD 185721). The typical peaks which indicate the tetragonality of tetrataenite FeNi (001) at 28.922° and (010) at 41.359° 2θ do not appear in

our measurement. The lattice parameters of both phases, austenite and ferrite, are not stoichiometric and indicate a mixture of Fe-Ni or Fe-C. The crystalline size of austenite is about 30 nm.

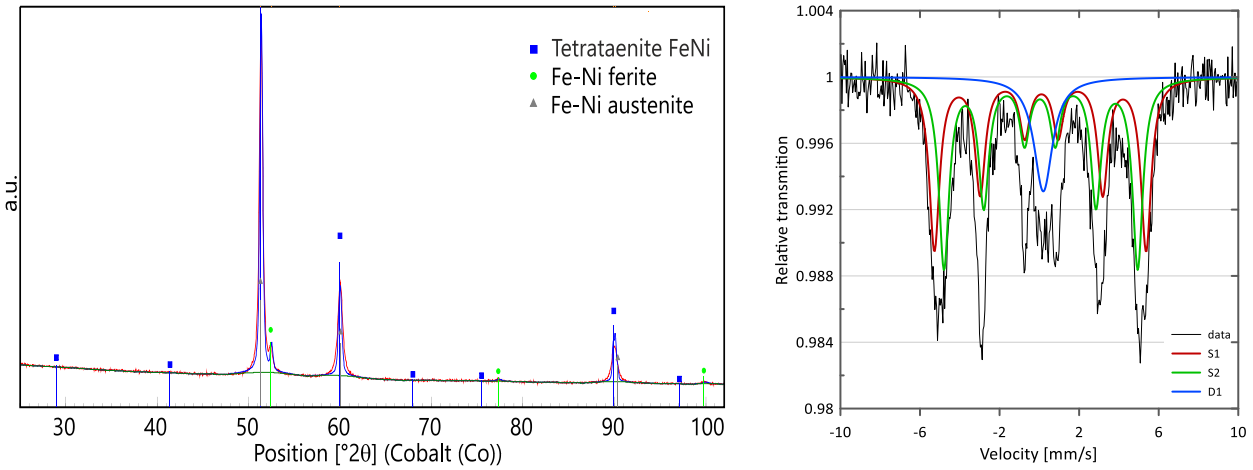

Figure 2 XRD pattern indicates the presence of ▲ Fe-Ni austenite and ● Fe-Ni ferrite, but the presence of ■ tetragonal FeNi is not confirmed (left); RT Mössbauer spectrum of Fe-Ni sample after reduction in hydrogen (right).

Mössbauer spectrum of the sample after reduction in hydrogen (320°C/ 20h) was fitted with three subspectra: two sextets and one singlet. The first sextet with the hyperfine induction B_{hf} = 33.2 T, IS = 0.047 mm/s, and relative content in the spectrum A = 0.34 (in atomic fraction of Fe atoms) can be associated with a bcc phase alfa-Fe(Ni). The second sextet with B_{hf} = 30.4 T, IS = 0.021 mm/s, and A = 0.54, can be ascribed to NiFe with ratio Fe:Ni close to Ni_3Fe alloy. The singlet with IS = 0.150 mm/s and A = 0.10 corresponds to paramagnetic FeNi particles.

The Zero Field Cooling (ZFC) and Field Cooling (FC) curves are drawn in **Figure 3** left. The ZFC curve starts at 4 K after cooling from 300 K in field <0.1 mT. After the cooling the external magnetic field was switched to 100 Oe and the magnetic moment was measured in this field with increasing temperature up to 300 K (the blue curve in **Figure 3**).

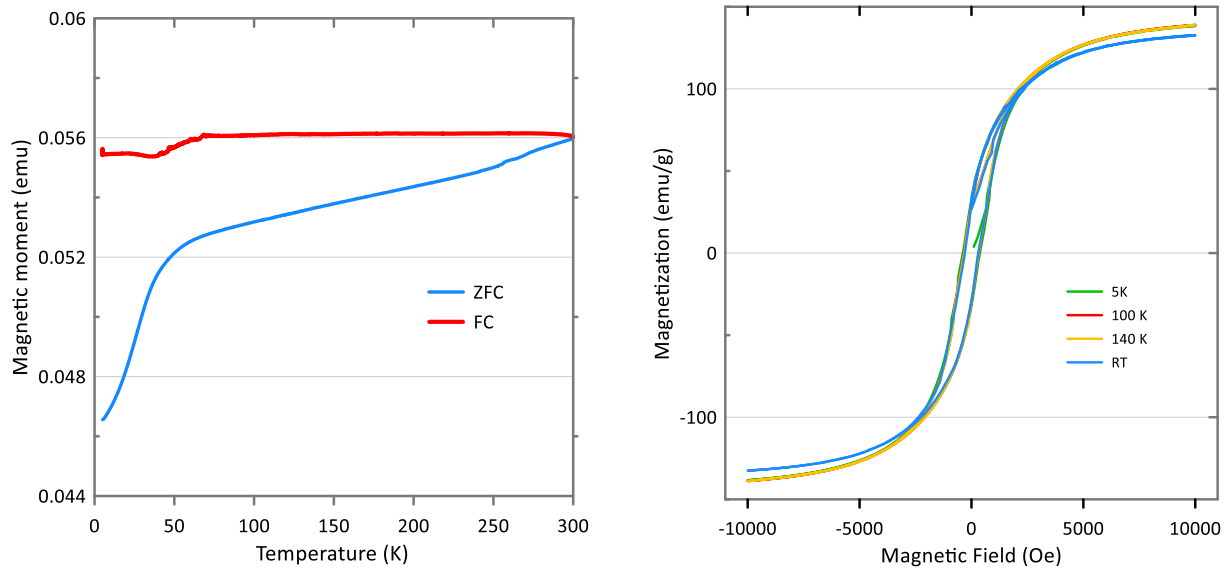

Figure 3 ZFC/FC curves for temperature dependences of magnetic moment (ZFC - Zero Field Cooling, FC - Field Cooling) (left) and magnetic hysteresis loops measured at 5, 100,140 K and RT (right).

After that, the FC measurement by decreasing temperature back up to 4 K in field 100 Oe was carried out (red curve in **Figure 3**). A comparison of both ZFC and FC curves indicates presence of superparamagnetic particle volumes in the measured sample with a blocking temperature about 40 K. The magnetic hysteresis loops were measured in magnetic field from 10000 to -10000 Oe at 5, 100 and 140 K (**Figure 3** right). The hysteresis loops overlap for given temperatures with saturation magnetization ~ 2.0 emu and coercivity 300 Oe. It is important that there are negligible changes in the loop parameters with increasing temperature. It could be explained by sample constitution in form of non-fixed powder particles.

4. CONCLUSION

The oxalate precipitation process successfully yielded a precursor comprising $Fe_{(1-X)}Ni_XC_2O_4.2H_2O$ particles. Through thermal decomposition at 320°C for 20 hours in a hydrogen atmosphere, porous FeNi particles with a size range of 1.2 - 1.5 µm were obtained. X-ray diffraction and Mössbauer spectroscopy analyses revealed the presence of a mixture of bcc phase α-Fe(Ni) and fcc Fe-Ni phase in the sample after thermal decomposition. Magnetic measurements indicated the existence of an antiferromagnetic phase, characterized by a Néel temperature (Tn) around 40 K.

ACKNOWLEDGEMENTS

This work has been created by financial support and using of the research infrastructure of the Institute of Physics of Materials Czech Academy of Sciences, v. v. i.; CzechNanoLab project LM2023051 funded by MEYS CR is gratefully acknowledged for the financial support of the measurements at CEITEC Nano Research Infrastructure.

REFERENCES

[1] CUI, J., KRAMER, M., ZHOU, L., LIU, F., GABAY, A., HADJIPANAYIS, G., BALASUBRAMANIAN, B., SELLMYER, D. Current progress and future challenges in rare-earth-free permanent Magnets. *Acta Materialia*. 2018, vol. 158, pp. 118-137. Available from: https://doi.org/10.1016/j.actamat.2018.07.049

[2] COEY, J.M.D. Pernament magnets: Plugging the gap. *Scripta Materialia.* 2012, vol. 67, pp. 524-529. Available from: https://doi.org/10.1016/j.scriptamat.2012.04.036

[3] GOLDSTEIN, J.I., HUSS, G.R., SCOTT, E.R.D. Ion microprobe analyses of carbon in Fe-Ni metal in iron meteorites and mesosiderites. *Geochimica et Cosmochimica Acta*. 2017, vol. 200, pp. 367-407. Available from: https://doi.org/10.1016/j.gca.2016.12.027

[4] ZHANG, J., WILLIAMS, D.B., GOLDSTEIN, J.I., CLARKE, R.S. Jr. Electron microscopy study of the iron meteorite Santa Catharina. *Meteoritics*. 1990, vol. 25, pp. 167-175. Available from: https://doi.org/10.1111/j.1945-5100.1990.tb00992.x

[5] NAYAK, B., MEYER, F.M. Tetrataenite in terrestrial rock. *American Mineralogist*. 2015, vol. 100, pp. 209-214. Available from: https://doi.org/10.2138/am-2015-5061

[6] MANDAL, S., DEBATA, M., SENGUPTA, P., BASU, S. $L1_0$ FeNi: a promising material for next generation permanent magnets. *Critical Reviews in Solid State and Materials Sciences*. 2022. Available from: https://doi.org/10.1080/10408436.2022.2107484

[7] NÉEL, L., PAULEVE, J., PAUTHENET, R., LAUGIER, J., DAUTREPPE, D. Magnetic properties of an iron-Nickel single crystal ordered by neutron bombardment. *Journal of Applied Physics*.1964, vol. 35, pp.873-876. Available from: https://doi.org/10.1063/1.1713516

[8] CHAMBEROD, A., LAUGIER, J., PENISSON, J.M. Electron irradiation effects on iron-nickel invar alloys, *Journal of Magnetism and Magnetic Materials.* 1979, vol.10, pp. 139-144. Available from: https://doi.org/10.1016/0304-8853(79)90165-3

[9] LEE, S., EDALATI, K., IWAOKA, H., HORITA, Z., OHTSUKI, T., OHKOCHI, T., KOTSUGI, M., KOJIMA, T., MIZUQUCHI, M., TAKANASHI, K. Formation of FeNi with L10-ordered structure using high-pressure torsion. *Philosophical Magazine Letters*. 2014, vol. 94, pp. 639-646. Available from: https://doi.org/10.1080/09500839.2014.955546

[10] MONTES-ARANGO, A.M., MARSHALL, L.G., FORTES, A.D., BORDEAUX, N.C., LANGRIDGE, S., BARMAK, K., LEWIS, L.H. Discovery of process-induced tetragonality in equiatomic ferromagnetic FeN., *Acta Materialia*. 2016, vol. 116, pp. 263-269. Available from: https://doi.org/10.1016/j.actamat.2016.06.050

[11] PEÑA RODRÍGUEZ, V.A., ROJAS-AYALA, C., MEDINA MEDINA, J., PAUCAR CABRERA, P., QUISPE-MARCATOMA, J., LANDAURO, C.V., ROJAS TAPIA, J., BAGGIO-SAITOVITCH, E.M., PASSAMANI, E.C. Fe50Ni50 synthesized by high energy ball milling: A systematic study using X-ray diffraction, EXAFS and Mössbauer methods. *Materials Characterization*. 2019, vol. 149, pp. 249-254. Available from: https://doi.org/10.1016/j.matchar.2019.01.036

[12] SATO, K.; SHARMA, P.; ZHANG, Y.; TTAKENAKA, K.; MAKINO, A. Crystallization Induced Ordering of Hard Magnetic L10 Phase in Melt-Spun FeNi-Based Ribbons*. AIP Advances*. 2016, vol. 6., article No. 055218. Available from: https://doi.org/10.1063/1.4952968

[13] KIM, J., KIM, S., SUH, J.Y., KIM, Y.J., KIM, Y.K., CHOI-YIM, H. Properties of a rare earth free L10-FeNi hard magnet developed through annealing of FeNiPC amorphous ribbons. *Current Applied Physics.* 2019, vol. 19, pp. 599-605. Available from: https://doi.org/10.1016/j.cap.2019.03.001

[14] IVANOV, Y.P., SARAC, B., KETOV, S.V., ECKERT, J., GREER, A.L. Direct Formation of Hard-Magnetic Tetrataenite in Bulk Alloy Castings. *Advanced Science.* 2022, vol. 10. Available from: https://doi.org/10.1002/advs.202204315

[15] LIMA, E. Jr., DRAGO, V., FICHTER, P.F.P., DOMINGUES, P.H.P. Tetrataenite and other Fe-Ni equilibrium phases produced by reduction of nanocrystalline $NiFe_2O_4$. *Solid State Communications.* 2003, vol.128, pp. 345-350. Available from: https://doi.org/10.1016/j.ssc.2003.08.046

[16] KURICHENKO, V.L., KARPENKOV, D.Y., KARPENKOV, A.Y., LYAKHOVA, M.B., KHOVAYLO, V.V. Synthesis of FeNi tetrataenite phase by means of chemical precipitation. *Journal of Magnetism and Magnetic Materials*. 2019, vol. 470, pp. 33-37. Available from: https://doi.org/10.1016/j.jmmm.2017.11.040

[17] ŽÁK, T., JIRÁSKOVÁ, Y. Confit: Mössbauer spectra fitting program. *Surface and Interface Analysis..* 2006, vol. 38, pp. 710-714. Available from: https://doi.org/10.1002/sia.2285

[18] D´ANTONIO, M.C., WLADIMIRSKY, A., PALACIOS, D., COGGOOLA, L., GONZÁLEZ-BARÓ, A.C., BARAN, E.J., MERCADER. R.C. Spectroscopic Investigations of Iron(II) and Iron(III) Oxalates. *Journal of the Brazilian Chemical Society*. 2019, vol. 20, No. 3, pp.445-450. Available from: https://doi.org/10.1590/S0103-50532009000300006

[19] ABRAS, A., FIGUEIREDO DE OLIVEIRA, E. Synthesis and Mössbauer study of iron oxalate coordination polymers of the type Fe(C2O4)(L) x (H2O)22−x. *Hyperfine Interactions*.1991, vol. Vol. 66, pp. 271-278. Available from: https://doi.org/10.1007/BF02395874

[20] RAMANI, SATHYAVATHIAMMA, M. P., PUTTASWAMY, N. G., MALLYA R. M. Mössbauer Effect Study of the Thermal Decomposition in Hydrogen of Homogeneously Mixed Ferrous Nickel Oxalates with Different Iron to Nickel Ratios. *Physica Status Solidi (a)*. 1983, vol. 77, issue 1, pp. 87 - 96. Available from: https://doi.org/10.1002/pssa.2210770110